BROAD-BAND *DOA* ESTIMATION AND BEAMFORMING IN MULTIPATH ENVIRONMENT

K. C. Indukumar and V. U. Reddy

Department of Electrical Communication Engineering
Indian Institute of Science, Bangalore - 560 012, INDIA

Abstract

Recently, Buckley [1] has developed orthogonal low-dimension models for broad-band sources and used them in ***DOA*** (direction of arrival) estimation and beamforming. The dimensionality of this low-dimension model is the number of significant eigenvectors of the source sample covariance matrix. When two or more sources impinge on the array, the dimensionality of the composite signal subspace is taken to be the sum of the dimensions of individual source representation spaces. This is the case when the sources are uncorrelated.

In this paper, considering a two-source model, we first show that the dimensionality of the composite signal subspace collapses when the signals from these sources are correlated, as it happens in the case of multipath, and the extent by which it collapses depends on the degree of correlation. Using the F-norm (Robenius norm) of the cross-correlation matrix of the direct and multipath signals as a measure of correlation between them, we illustrate how the norm decreases as the delay increases, indicating that the degree of correlation falls with delay. We propose spatial smoothing for reducing the norm and show that the norm decreases to zero asymptotically with the number of subarrays. We then derive an analytical expression for an upper bound on the F-norm and using this, we study the effect of spacing and directions of the sources on the rate of decorrelation with progressive smoothing.

Simulations are provided to illustrate the impact of progressive smoothing on ***DOA*** estimation and beamforming performance.

1 INTRODUCTION

Subspace based methods of ***DOA*** (direction of arrival) estimation, pioneered by Pisarenko [2], and generalised by Schmidt [3] and Bienvenu [4] for narrowband signals, have been recently extended to broad-band case by Buckley [1,5], Buckley and Griffiths [6] and, Wang and Kaveh [7]. In [1], Buckley has developed low-dimension models for the broad-band sources, termed as broad-band representation spaces, and used these models in ***DOA*** estimation and beamforming. As defined in [1], the dimensionality of the broad-band source representation space is the number of significant eigenvectors of the source sample covariance matrix, which may also be viewed as the effective rank of this matrix. When several sources impinge on the array, the dimensionality of the composite signal subspace, which represents all the impinging sources, is taken to be the sum of the dimensions of the individual source representation spaces. This implicitly assumes that the impinging signals are uncorrelated.

There are situations when several or all of the impinging signals are correlated, e.g., multipath propagation and smart jamming environments. In multipath propagation, the signal arrives via a direct and reflected paths and the *DOA*s of these signals are in general different. The signal arriving via the reflected path (which we refer to as the multipath signal) can be viewed as the signal emitted from another source that is correlated with the one associated with the direct path. The delay between the two signals, i.e., the difference between the times of arrival of the direct and reflected signals, as observed at the reference sensor of the array, depends on the path lengths of these two signals. Recently, the ***DOA*** estimation performance of the subspace-based methods and the performance of the linearly constrained *MV* (minimum variance) beamformer in the presence of multipath have been extensively analysed in the case of narrowband signals [8,9,10,11]. In particular, subarray averaging has been proposed in [8] and [9], and the impact of progressive smoothing (averaging with increasing number of subarrays) has been analysed in [10] and [11].

In this paper, we first show that in the presence of multipath, the dimensionality of the composite signal subspace collapses and the extent by which it collapses depends on the amount of multipath delay. We show this by choosing a two-source model with the two sources corresponding to the signals arriving via the direct and reflected paths. We use the F-norm (Robenius norm) of the cross-correlation matrix of the data sample vectors of these signals as a measure of correlation between them and show that this norm decreases as the delay between the two signals increases. Next, we show that the dimensionality of the signal subspace is restored with subarray averaging. However, the restoration of this dimensionality does not mean that the correlation between the two signals has reduced to zero. The significant residual correlation which is still left between these signals affects the *DOA* estimation performance in finite data case and interference rejection performance of the *MV* beamformer even in the infinite data case. We illustrate this with a few examples in Section 5.

To study the effect of progressive smoothing on the correlation, we derive an expression for the upper bound on the F-norm of the cross-correlation matrix which shows that the norm tends to zero asymptotically with the number of subarrays indicating that the correlation falls to zero only asymptotically. The effect of spacing and directions of the sources on the rate of decorrelation with progressive smoothing is also broughtout by this bound. Simulation results are provided to support our assertions.

We may point out here that we chose the two-source signal model to keep the notation and the analysis simple. The results, however, extend to arbitrary number of sources.

2 BACKGROUND

Consider a linear [1] array with Misotropic sensors and a tapped delay line with K taps attatched to each sensor (see ***Fig. 1***). Assume that two broad-band sources are impinging on the array from two directions θ_d and θ_s , and let $d(t)$ and $s(t)$ be the signals emitted by these sources. Let $\mathbf{X}(t)$ denote the KM dimensional stacked vector formed from K delayed array output vectors as given below

$$\mathbf{X}(t) = [\chi_1^T(t), \chi_2^T(t), \ldots, \chi_K^T(t)]^T \tag{2.1}$$

where

$$\chi_k(t) = [x_{1k}(t), x_{2k}(t), \ldots, x_{Mk}(t)]^T \tag{2.2}$$

This work is supported in part by Electronics and Radar Development Establishment, Bangalore 560 093, INDIA

[1] Though the assumption of linear array is not required in obtaining some results of the paper such as, collapse of signal subspace dimensionality in the presence of multipath and the interpretation of the F-norm of cross-correlation matrix as a measure of the correlation, it is essential for spatial smoothing and therefore, we assume a linear array through out the paper.

CH2882-9/90/0000-0532$1.00 © (1990 IEEE)

Here, $x_{mk}(t)$ denotes the signal from element m at k-th tap at time instant t. The vector $\mathbf{X}(t)$ is also termed as the array snapshot vector at time t. We can decompose $x_{mk}(t)$ as

$$x_{mk}(t) = d_{mk}(t) + s_{mk}(t) + v_{mk}(t) \tag{2.3}$$

where $d_{mk}(t)$ and $s_{mk}(t)$ are the components due to the signals arriving from θ_d and θ_s, respectievely, and $v_{mk}(t)$ is the component due to the additive sensor noise which is assumed to be uncorrelated with the sources and also to be spatially white. Assuming the first sensor element to be the reference element, we can express

$$d_{mk}(t) = d(t - (\mathrm{m}-1)T_d - (k-1)T_o) \tag{2.4}$$

$$s_{mk}(t) = s(t - (\mathrm{m}-1)T_s - (k-1)T_o) \tag{2.5}$$

where T_d and T_s are the inter-element propagation delays

$$T_d = \frac{A}{\mathrm{c}} sin\theta_d, \qquad T_s = \frac{A}{c} sin\theta_s \tag{2.6}$$

with A denoting the element spacing and c denoting the velocity of propagation, and T_o is the delay between taps. Since the noise is assumed to be independent from sensor to sensor, we can express

$$v_{mk}(t) = v_m(t - (k-1)T_o) \tag{2.7}$$

The MK by MK sample data covariance matrix is given by

$$\Phi = E[\mathbf{X}(t)\mathbf{X}^{+}(t)] \tag{2.8}$$

which, in view of (2.3), can be expressed as

$$\Phi = \Phi_{dd} + \Phi_{ss} + \Phi_{ds} + \Phi_{sd} + \Phi_{vv} \tag{2.9}$$

where Φ_{dd}, Φ_{ss} and Φ_{vv} refer to the sample covariance matrices of source signals and the noise. From (2.1) and (2.2), it follows that Φ can be partitioned into K^2 submatrices, each of M x M elements. Each submatrix represents the covariance matrix $E[\chi_k(t)\chi_j^{+}(t)], 1 \leq k, j \leq K$, where $\chi_k(t)$ is a M-dimensional array output vector. We refer to this as the $kj-th$ submatrix.

In view of (2.2) and (2.3), we can express the mn-th element in kj-th submatrix of Φ_{dd} as

$$[\Phi_{dd_{mn}}]_{kj} = R_{dd}((n-m)T_d + (j-k)T_o) \tag{2.10}$$

Similarly, we have

$$[\Phi_{ss_{mn}}]_{kj} = R_{ss}((n-m)T_s + (j-k)T_o) \tag{2.11}$$

and

$$[\Phi_{ds_{mn}}]_{kj} = R_{ds}((n-1)T_s - (m-1)T_d + (j-k)T_o) \tag{2.12}$$

with

$$[\Phi_{sd_{mn}}]_{kj} = [\Phi_{ds_{nm}}]^{*}_{jk} \tag{2.13}$$

The last relation follows from the fact that Φ_{sd} is Hermetian transpose of Φ_{ds}, i.e., $\Phi_{sd} = \Phi_{ds}^{+}$. Finally, the mn-th element in kj-th submatrix of Φ_{vv} is given by

$$[\Phi_{vv_{mn}}]_{kj} = \begin{cases} R_{vv}((j-k)T_o) & , \ m = n \\ 0 & , \ m \neq n \end{cases} \tag{2.14}$$

If $d(t)$ and $s(t)$ are the signals from uncorrelated sources, the cross-covariance matrices @& and Φ_{sd} vanish. In multipath environment, however, one signal is a delayed version of the other, assuming a pure delay environment. If we consider $s(t)$ to be the multipath signal with path delay T_α, we have

$$s(t) = d(t - T_\alpha) \tag{2.15}$$

The elements of Φ_{ds} (and also of Φ_{sd}) are then modified as

$$[\Phi_{ds_{mn}}]_{kj} = R_{dd}(T_\alpha + (n-1)T_s - (m-1)T_d + (j-k)T_o) \tag{2.16}$$

We now assume that $d(t), s(t)$ and $v(t)$ are all zero mean, bandlimited random processes with flat power spectral densities over a bandwidth $\Delta\omega$ centered at frequency ω_o. Let the powers in these signals be denoted by σ_d^2, σ_s^2 and σ_v^2, respectievely. Then

$$R_{dd}(r) = \sigma_d^2 sinc\left(\frac{\Delta\omega\tau}{2}\right)\exp(i\omega_o r) \tag{2.17}$$

and, $R_{ss}(r)$ and $R_{vv}(r)$ are same as (2.17) with σ_d^2 replaced by σ_s^2 and σ_v^2, respectievely, and

$$R_{ds}(r) = \sigma_d\sigma_s sinc\left(\frac{\Delta\omega\tau}{2}\right)\exp(i\omega_o r) \tag{2.18}$$

where $sinc(\cdot)$ denotes the $sinc$ function

$$sinc(\alpha) = \frac{\sin\alpha}{\alpha} \tag{2.19}$$

and i in the exponent denotes $\sqrt{-1}$. Following Compton [12], we express the correlation functions in terms of normalised parameters.

Denote the relative bandwidth of the signals as B_d, i.e., $B_d = \Delta\omega/\omega_o$, and express the multipath delay T_α as r times the inverse of the signal bandwidth, i.e., $T_\alpha = 2\pi r/\Delta\omega$, where r is any real number. We choose the element spacing as one half of the wavelength corresponding to the center frequency ω_o, and the delay between taps as specified by the sampling theorem for bandpass signals. That is, $T_o = 1/f_s$ with $f_s = 2f_{max}/\lfloor f_{max}/\Delta f \rfloor$ where $\lfloor x \rfloor$ denotes the largest integer not exceeding x [14]. The mn-th element of kj -th submatrix of Φ_{dd} is then expressed as

$$\begin{aligned}[\Phi_{dd_{mn}}]_{kj} \ = \ & \sigma_d^2 sinc\left(\frac{B_d}{2}(\pi(n-m)sin\theta_d + \omega_o T_o(j-k))\right) \\ & \exp(i(\pi(n-m)sin\theta_d + \omega_o T_o(j-k))) \end{aligned} \tag{2.20}$$

The corresponding elements of Φ_{ss} and Φ_{vv} can be similarly expressed.

2.1 Dimensionality of the Source Representation Space

As defined in [1], a source representation space is the span of eigenvectors associated with 'D' significant eigenvalues of the corresponding source sample covariance matrix. For example, the span of 'D' eigenvectors of Φ_{dd} is the source representation space associated with the signal $d(t)$. The value of D can also be viewed as the effective dimension of the signal subspace. If $\lambda_j, j = 1, 2, \cdots, MK$, denote the ordered eigenvalues of the matrix Φ_{dd}, then D is the smallest value for which

$$\frac{\sum_{j=1}^{D}\lambda_j}{Trace(\Phi_{dd})} \geq 99.99\%$$

If D_1 and D_2 represent the effective dimensions of the individual signal subspaces associated with $d(t)$ and $s(t)$, then $D_1 + D_2$ is the dimension of the composite signal subspace, i.e., $(D_1 + D_2)$ eigenvectors of $(\Phi_{dd} + \Phi_{ss})$ associated with $(D_1 + D_2)$ ordered eigenvalues span the composite signal subspace.

2.2 *MV* Beamforming

In a linearly constrained minimum variance (MV) beamformer, the array signals are combined so as to pass the desired directional signal to the output without distortion while maximally rejecting the signals from other directions. We consider Frost beamformer [13] with desired signal in the broad-side direction. Let $\mathbf{W}$ denote the weight vector formed by stacking the tap weights column-wise, i.e.,

$$\mathbf{W} = [w_{11}, w_{21}, \cdots, w_{1K}, w_{2K}, \cdots, w_{MK}]^T \tag{2.21}$$

The optimum weight vector is given by [13]

$$\mathbf{W}_{opt} = \Phi^{-1}C[C^T\Phi^{-1}C]^{-1}\mathcal{F} \tag{2.22}$$

where C is the MK by K constraint matrix and ? is K by **1** constraint response vector **as** defined in [**13**]. The interference rejection performance of the beamformer is then specified by depth of the null in the interference direction in the output beampattern given by $\mathbf{W}_{opt}^{+}\mathbf{a}(\theta,\omega)$, where $\mathbf{a}(\theta,\omega)$ is the MK-dimensional steering vector at a frequency **w**.

2.3 *DOA* Estimation

As suggested in [1], we perform eigen decomposition of the prewhitened data covariance matrix, $\Phi_{vv}^{-\frac{1}{2}}\Phi(\Phi_{vv}^{-\frac{1}{2}})^{+}$, and construct noise subspace E_n from the eigenvectors $\mathbf{e}_{D+1},\cdots,\mathbf{e}_{KM}$, associated with the last $KM-D$ eigenvalues of the prewhitened matrix, where D is known a priori **or** estimated from the time-bandwidth products of the signals [**1**]. We note here that the noise statistics are assumed to be known a priori.

In view of the prewhitening of the data covariance matrix, the source observations are altered by the corresponding transformation. We therefore use a transformed location vector

$$\mathbf{b}(\theta,\omega)=\Phi_{vv}^{-\frac{1}{2}}\mathbf{a}(\theta,\omega) \tag{2.23}$$

and compute the spatial spectrum **as** [**6**]

$$P(\theta)=\sum_{k=1}^{N_f}\frac{1}{\sum_{i=D+1}^{MK}|\,\mathbf{b}^{+}(\theta,\omega_k)\mathbf{e}_i\,|^2} \tag{2.24}$$

where N_f denotes the number of equispaced frequencies in the bandwidth of the signal over which the spectrum is averaged. Location of the peaks in $P(\theta)$ are taken **as** the estimates of the DOAs of the impinging sources.

3 EFFECT OF MULTIPATH DELAY AND F-NORM OF $(\Phi_{ds}+\Phi_{sd})$

When the impinging signals are uncorrelated, the effective dimension of the composite signal subspace is the sum of the dimensions of the individual source representation spaces. But, when the signals are correlated **as** in multipath, the effective dimension falls and we refer to this **as** the collapse in the dimensionality of the signal subspace. The extent by which it collapses depends on the multipath delay.

We note from **(2.16)** and **(2.17)** that the correlation between the direct signal and its multipath decreases **as** the path delay increases. We also note that **as** T_α increases, the magnitude of each element of the cross-correlation matrix decreases, suggesting that we **use** the F-norm of this matrix **as** a measure of correlation between the direct and multipath signals. In the limit, **as** the path delay, T_α, tends to infinity, the F- norm, $\|\,\Phi_{ds}+\Phi_{sd}\,\|_F$, tends to zero which corresponds to the uncorrelated case.

To illustrate the above phenomena, we considered a scenario with one signal arriving from 0° and the other from **10°**, $M=6$ and $K=4$. The direct signal $d(t)$ and the multipath signal $s(t)$ were assumed to arrive from 0° and 10°, respectively. The relative bandwidth of the signals was chosen **as** 0.4, and this fixed the value of To **as** $\omega_o T_o=2.5\pi$. The delay of the multipath signal, T_α, was taken **as** $\frac{2\pi r}{\Delta\omega}$, where **r** can assume any real value. The signal and noise powers were set at $0\,dB$, i.e., $\sigma_d^2=\sigma_s^2=\sigma_v^2=1$. Table 1 gives the effective dimension of the composite signal subspace, which is computed **as** described in the previous section. and the **F-** norm for several values of **r.**

Table **1.** Effect of multipath delay on D and F-norm $(T_\alpha=\frac{2\pi r}{\Delta\omega})$

r	D of ($\Phi_{dd}+\Phi_{ss}$ $+\Phi_{ds}+\Phi_{sd}$)	$\|\,\Phi_{ds}+\Phi_{sd}\,\|_F$
0.1	5	24.21
		19.48
		15.89
0.4	5	19.48
1	6	15.89
3	8	3.152
*	8	0

We note from the results of the table that though the signal subspace dimension for $\mathbf{r}=3$ is same **as** that for the uncorrelated case, the F-norm is non-zero indicating that there is still some residual correlation left between the two signals. We know from the analysis of the MV beamformer for narrowband signals [**11**] that the interference rejection performance degrades if the interference is correlated with the desired signal and the extent of degradation depends on the amount of correlation. To show that the value of the F-norm indicates a residual correlation and hence a proportional degradation in the performance of the MV beamformer **as** in the narrowband case, we used the above array for MV beamforming treating $d(t)$ **as** the desired signal and $s(t)$ **as** the inteference. The noise power was fixed same **as** before, but the signal powers were set at $10\,dB$ each. The optimum weight vector was computed using **(2.22)with** the constraint response vector **as** $\mathcal{F}=[\,1,0,\cdots,0]^T$, and the beampattern was evaluated at the center frequency of the band. Note from the inset in ***Fig.* 2** that the null depth (at 10°) in the beampattern increases with **r** and for $\mathbf{r}=3$ it is still $13\,dB$ less than that of the uncorrelated case. This confirms our assertion that the F-norm can be used **as** the measure of Correlation.

4 EFFECT OF PROGRESSIVE SPATIAL SMOOTHING ON DECORRELATION OF THE SOURCES

In this section, we first show that F-norm of the cross-correlation matrix tends to zero asymptotically with progressive sub array averaging (progressive smoothing) and then derive an upper bound on the F-norm. Using this bound, we study the effect of spacing and directions of the sources on the rate of decorrelation with progressive smoothing. We give some numerical results to show that the bound and actual value of F-norm have similar shapes.

Assume that the linear array given in ***Fig.* 1** is extended by augmenting with additional sensors and tapped delay lines with K taps, and the extended array is grouped into overlapping subarrays of size M, with a K-tap delay line attached to each sensor. Let $\mathbf{X}^l(t)$ denote the KM-dimensional stacked data vector of I- th subarray, formed from K delayed array output vectors similar to **(2.1)** and **(2.2).** Following the notation of Section **2** and assuming $s(t)=d(t-T_\alpha)$, the mk-th element of $\mathbf{X}^l(t)$ can be expressed **as**

$$\begin{aligned}x_{l+m-1,k}(t) &= d(t-(\mathrm{I}+\mathrm{m}-2)T_d-(k-1)T_o)\\ &\quad +d(t-T_\alpha-(\mathrm{I}+\mathrm{m}-2)T_s-(k-1)T_o)\\ &\quad +v_{l+m-1}(t-(k-1)T_o)\\ &\quad \forall\,1\le m\le M,1\le k\le K\end{aligned} \tag{4.1}$$

The MK by MK sample covariance matrix of I-th subarray is then given by

$$\Phi^l=\Phi_{dd}+\Phi_{ss}+\Phi_{ds}^l+\Phi_{sd}^l+\Phi_{vv} \tag{4.2}$$

where we have shown the dependence on the position of the subarray in the cross-correlation term only, which can be verified easily. The mn-th element in kj-th submatrix of Φ_{ds}^l can be shown to be

$$[\Phi_{ds_{mn}}^l]_{kj}=R_{dd}(T_\alpha+(n-2)T_s-(m-2)T_d+(j-k)T_o+l(T_s-T_d)) \tag{4.3}$$

Denote the spatially smoothed covariance matrix with L subarrays (which we refer to **as** L smoothing steps) **as**

$$\bar{\Phi}^L=\frac{1}{L}\sum_{l=1}^{L}\Phi^l \tag{4.4}$$

In view of **(4.2)**, we get

$$\bar{\Phi}^L=\Phi_{dd}+\Phi_{ss}+\Phi_{vv}+\frac{1}{L}\sum_{l=1}^{L}(\Phi_{ds}^l+\Phi_{sd}^l) \tag{4.5}$$

Note that since the lag value τ increases with I (see **(4.3))** and the magnitude of the autocorrelation value decreases with τ (see **(2.17)**),

No: of subarrays L	two-source case	three-source case
1	5	5
2	8	10
3		12
*	8	12

Note from the results of the table that the dimensionality of the signal subspace collapses when the multipath delay is small causing the impinging sources to be highly correlated, and with subarray averaging, we recover this dimensionality. In the examples considered here, the number of subarrays required for restoring the dimensionality is 2 and 3, respectievely, for the two- and three-source cases.

From (4.3) and the assumption that $d(t)$ is a bandlimited random process, we can show that

$$\left[\left(\frac{1}{L}\sum_{l=1}^{L}(\Phi_{ds}^{l}+\Phi_{sd}^{l})\right)_{mn}\right]_{kj} =$$

$$\frac{\sigma_d^2}{\Delta\omega L}\int_{\omega_o-\Delta\omega/2}^{\omega_o+\Delta\omega/2}\exp\left(i\omega(j-k)T_o\right)\left(\frac{sin\omega L(T_s-T_d)/2}{sin\omega(T_s-T_d)/2}\right)$$

$$\left(\exp\left(i\omega(T_\alpha+(n-2)T_s-(m-2)T_d+\frac{L+1}{2}(T_s-T_d))\right)\right.$$

$$\left.+\exp\left(-i\omega(T_\alpha+(m-2)T_s-(n-2)T_d+\frac{L+1}{2}(T_s-T_d))\right)\right)d\omega \qquad (4.6)$$

where we assumed a pure delay environment for simplicity. Applying Schwarte inequality to the integrand in (4.6) and simplifying, we obtain (after some work) (see Appendix A)

LHS of (4.6)$\leq$

$$\left[\frac{\sigma_d^2}{L}\left(1+\frac{2cos(2\omega_oT_\alpha+(m+n-3+L)\beta)\ sin((B_d/2)(2\omega_oT_\alpha+(m+n-3+L)\beta)}{B_d(2\omega_oT_\alpha+(m+n-3+L)\beta)}\right.\right.$$

$$\frac{2cos(\beta L)\ sin((B_d/2)\beta L)}{B_d\beta L}$$

$$\frac{cos(2\omega_oT_\alpha+(m+n-3)\beta)\ sin((B_d/2)(2\omega_oT_\alpha+(m+n-3)\beta))}{B_d(2\omega_oT_\alpha+(m+n-3)\beta)}$$

$$\left.\left.-\frac{cos(2\omega_oT_\alpha+(m+n-3+2L)\beta)\ sin((B_d/2)(2\omega_oT_\alpha+(m+n-3+2L)\beta))}{B_d(2\omega_oT_\alpha+(m+n-3+2L)\beta)}\right)^{\frac{1}{2}}\right.$$

$$\left.\left(\frac{2}{B_d\beta}\left(cot\frac{\beta}{2}(1-\frac{B_d}{2})-cot\frac{\beta}{2}(1+\frac{B_d}{2})\right)\right)^{\frac{1}{2}}\right] \qquad (4.7)$$

where $\beta=\omega_o(T_s-T_d)$. The bound on the F-norm of the smoothed cross-correlation matrix is then given by

$$\|\frac{1}{L}\sum_{l=1}^{L}(\Phi_{ds}^{l}+\Phi_{sd}^{l})\|_F\leq K\sqrt{\sum_{m=1}^{M}\sum_{n=1}^{M}(RHS of (4.7))^2} \qquad (4.8)$$

Fig. 3 gives the plots of the bound (RHS of (4.8)) and the true value of the F-norm (LHS of (4.8)), for 3 different source configurations, $(0^o,10^o),(0^o,30^o)$ and $(50^o,60^o)$, as a function of the smoothing index. The plots bring out the following:

1. The bound depicts all the essential features, like the rate of fall with L, sidelobe nature caused by the $\frac{sinx}{x}$ shape of the correlation function etc.
2. The rate of fall is higher when the sources are widely spaced (plots 1 and 2)
3. The rate of fall is slower when the sources are away from the broad-side direction (plots 1 and 3).

As the F-norm reflects the effective correlation between the direct and multipath signals, we note from the plots that the rate of decorrelation with smoothing is faster when the sources are widely spaced and is slower when the sources are away from the broad-side direction.

In the next section, we give several simulation results which illustrate the impact of progressive smoothing on both DOA estimation and MV beamforming. In particular, we show that DOA estimation performance improves with progressive smoothing in the finite data case and the rate of this improvement is higher in the case where the rate of fall in the F-norm is larger. We give asymptotic beampatterns for several values of L to show that the interference rejection performance goes up when the norm goes down and vice versa, thus confirming our assertion that the F-norm is a measure of the effective correlation between the two signals.

5 SIMULATION RESULTS

To support our assertions on the impact of progressive smoothing, we conducted simulations on DOA estimation and MV beamforming. *Fig.* 4 shows the DOA estimation performance for different degrees of smoothing for two senarios, $(0^o, 10^o)$ and $(0^o, 30^o)$. In each case, the signal and noise powers were all set at $0dB$ and the covariance matrices were estimated from 200 snapshots of data. The value of r in T_α was chosen as 0.4, and the relative bandwidth B_d was fixed at 0.4. The spatial spectrum was computed from (2.24) choosing $N_f=3$.

The plots of *Fig.* 4 (a) show that the DOA estimation performance improves progressievely with smoothing. The plots for $L=2$, corresponding to the two scenarios, show that for the same degree of Smoothing, the rate of improvement is higher in the case of widely spaced sources. This is what we predicted from the F-norm curves of *Fig.* 3. Note that DOA estimation fails with $L=1$ in both cases.

To illustrate the effect of progressive smoothing on the interference rejection performance of the MV beamformer and also to demonstrate that the residual F-norm of the cross-correlation matrix is the measure of the residual correlation between the impinging signals, we computed beampatterns for various degrees of smoothing and plotted the results in *Fig.* 5. The beampattern was evaluated at the center frequency of the band as described in Section 2.2 replacing Φ in (2.22) with Φ^L. The scenarios, the signal bandwidths, the multipath delay and the subarray size were same as those used in DOA estimation (see *Fig.* 4) excepting that the signal powers were set at $10dB$ each. In each case, the signal arriving from 0^o was assumed to be the desired signal and the multipath signal was treated as the interference. The plots of *Fig.* 5 depict the following.

1. There is a one-to-one correspondence between the increase (and decrease) in the null depth and the decrease (and increase) in the F-norm with L. For example, for the scenario (0^o, 10^o)

(Fig. 5(a)), the null depth progressievely increases when L is increased from 1 to 4 and from 4 to 12, but reduces for $L = 15$ (see the inset). The F-norm for the corresponding scenario (plots 1 in Fig. 3) shows opposite behaviour implying that the residual F-norm is the measure of the residual correlation , since the degradation in the interference rejection performance is proportional to the correlation [11].

2. **The** rate of increase in the null depth with L is higher for widely spaced sources for which case the rate of fall in the F-norm is larger. This can be seen from the beampatterns for $L = 1$ and 4 for the two scenarios (see Fig. 5) and the corresponding F-norm plots in Fig. 3 (plots 1 and 2).

6 CONCLUSIONS

In this paper, we have shown that the effective dimension of the signal subspace collapses in the presence of multipath and it can be recovered with subarray averaging. We have proposed the F-norm of the cross-correlation matrix **as** a measure of the correlation between the impinging signals and derived an upper bound on this norm which depicts all the essential features of the true F-norm. Using this bound we studied how the correlation between the direct and multipath signals falls with progressive smoothing and how the rate at which it falls depends on the spacing and directions of the sources. Computer simulations have been provided to support our theoretical predictions.

To keep the notation and the analysis simple, our analysis was restricted to two-source models. However, the results extend to the signal models with more than two sources.

A APPENDIX

Applying Schwartz inequality

$$\int_a^b f(x)g(x)dx \le \left(\int_a^b |f(x)|^2\,dx\right)^{\frac{1}{2}} \left(\int_a^b |g(x)|^2\,dx\right)^{\frac{1}{2}}$$

to the integrand in Equation (4.6), we get
LHS of (4.6) $\le$

$$\left(\int_{\omega_o-\frac{\Delta\omega}{2}}^{\omega_o+\frac{\Delta\omega}{2}} \left|\left(\frac{\sigma_d^2}{\Delta\omega L}\right) sin\omega L\left(\frac{T_s-T_d}{2}\right)\right.\right.$$

$$\left(\exp\left(i\omega\left(T_\alpha+(n-2)T_s-(m-2)T_d+\frac{L+1}{2}(T_s-T_d)\right)\right)+\right.$$

$$\left.\left.\exp\left(-i\omega\left(T_\alpha+(m-2)T_s-(n-2)T_d+\frac{L+1}{2}(T_s-T_d)\right)\right)\right|^2 d\omega\right)^{\frac{1}{2}}$$

$$\left(\int_{\omega_o-\Delta\omega/2}^{\omega_o+\Delta\omega/2} \left|\frac{1}{sin\omega\left((T_s-T_d)/2\right)}\right|^2 d\omega\right)^{\frac{1}{2}} \qquad (A.1)$$

Taking the magnitude square of the term in the first integrand of RHS of (A.1) gives
RHS of (A.l) =

$$\left(\int_{\omega_o-\Delta\omega/2}^{\omega_o+\Delta\omega/2} \left(\frac{\sigma_d^2}{\Delta\omega L}\right)^2 sin^2\omega L\left(\frac{T_s-T_d}{2}\right)\right.$$

$$\left(\left(cos\omega\left(T_\alpha+(n-2)T_s-(m-2)T_d+\frac{L+1}{2}(T_s-T_d)\right)\right.\right.$$

$$+cos\omega\left(T_\alpha+(m-2)T_s-(n-2)T_d+\frac{+1}{2}(T_s-T_d)\right)\Big)^2$$

$$\left.\left.+\left(sin\omega\left(T_\alpha+(n-2)T_s-(m-2)T_d+\frac{L+1}{2}(T_s-T_d)\right)\right.\right.\right.$$

$$\left.\left.\left.-sin\omega\left(T_\alpha+(m-2)T_s-(n-2)T_d+\frac{L+1}{2}(T_s-T_d)\right)\right)^2 d\omega\right)^{\frac{1}{2}}$$

$$\left(\int_{\omega_o-\frac{\Delta\omega}{2}}^{\omega_o+\frac{\Delta\omega}{2}} cosec^2\omega\left(\frac{T_s-T_d}{2}\right)d\omega\right)^{\frac{1}{2}} \qquad (A.2)$$

which can be simplified to
RHS of (A.2) =

$$\left(\int_{\omega_o-\frac{\Delta\omega}{2}}^{\omega_o+\frac{\Delta\omega}{2}} \left(\frac{\sigma_d^2}{\Delta\omega L}\right)^2 sin^2\omega L\left(\frac{T_s-T_d}{2}\right)\right.$$

$$\left.cos^2\frac{\omega}{2}\left(2T_\alpha+(m+n-3+L)(T_s-T_d)\right)d\omega\right)^{\frac{1}{2}}$$

$$\left(\int_{\omega_o-\Delta\omega/2}^{\omega_o+\Delta\omega/2} cosec^2\omega\left(\frac{T_s-T_d}{2}\right)d\omega\right)^{\frac{1}{2}} \qquad (A.3)$$

Evaluating the integral in (A.3) and simplifying , we obtain
RHS of (A.3) =

$$\frac{\sigma_d^2}{\Delta\omega L}\left[\left(\Delta\omega+2cos\left(\omega_o\left(2T_\alpha+(m+n-3+L)\ (T_s-T_d)\right)\right)\right.\right.$$

$$\frac{sin\left(\frac{\Delta\omega}{2}\left(2T_\alpha+(m+n-3+L)\ (T_s-T_d)\right)\right)}{2T_\alpha+(m+n-3+L)\ (T_s-T_d)}$$

$$-\frac{2cos\left(\omega_o L\left(T_s-T_d\right)\right)\ sin\left(\frac{\Delta\omega}{2}\left(T_s-T_d\right)\right)}{L\left(T_s-T_d\right)}$$

$$-cos\left(\omega_o\left(2T_\alpha+(m+n-3)\ (T_s-T_d)\right)\right)$$

$$\frac{sin\left(\frac{\Delta\omega}{2}\left(2T_\alpha+(m+n-3)\ (T_s-T_d)\right)\right)}{2T_\alpha+(m+n-3)\ (T_s-T_d)}$$

$$-cos\left(\omega_o\left(2T_\alpha+(m+n-3+2L)\ (T_s-T_d)\right)\right)$$

$$\left.\frac{sin\left(\frac{\Delta\omega}{2}\left(2T_\alpha+(m+n-3+2L)\ (T_s-T_d)\right)\right)}{2T_\alpha+(m+n-3+2L)\ (T_s-T_d)}\right)^{\frac{1}{2}}$$

$$\left(\frac{2}{(T_s-T_d)}\left(cot\left(\left(\frac{T_s-T_d}{2}\right)\left(\omega_o-\frac{\Delta\omega}{2}\right)\right)\right.\right.$$

$$\left.\left.-\cot\left(\left(\frac{T_s-T_d}{2}\right)\left(\omega_o+\frac{\Delta\omega}{2}\right)\right)\right)^{\frac{1}{2}}\right] \qquad (A.4)$$

Substituting $\frac{\Delta\omega}{\omega_o} = B_d$ and $\omega_o(T_s-T_d) = \beta$ in (A.4) gives the R.H.S of (4.7).

REFERENCES

1. Buckley, K.M., " A Source Representation ⋯ ," *Ph.D.* dissertation, Dept. of Elec. Eng., USC, July 1986.
2. Pisarenko, V.F., " The Retrieval ⋯," Geophys. *J.* Royal Astronomical *Soc.*, pp. 347-366,1973.
3. Schmidt, R.O., " Multiple Emitter ⋯," Proc. RADG Spec. Eat. Workshop *(Griffis* AFB, *N.Y)*, pp. 243-258, 1979.
4. Bienvenu, G. and L. Kopp, " Adaptivity to ⋯," Proc. *of* ICASSP, pp. 307-310, 1980.
5. Buckley, K.M., " Spatial/Spectral ⋯," IEEE Trans. **on** ASSP, pp. 249-266, March 1987.
6. Buckley, K.M. and L.J. Griffiths, " Broad-Band ⋯," IEEE Trans. **on** ASSP, pp. 953-964, July 1988.
7. Wang, H. and M. Kaveh, " Coherent Signal ⋯," IEEE Trans. **on** ASSP, pp. 823-831, August 1985.
8. Shan, **T.J.**, M. Wax and T. Kailath, " On Spatial ⋯ ," IEEE Trans. **on** *ASSP*, pp. 806-811, August 1985.
9. Shan, T.J. and T. Kailath, " Adaptive beamforming ⋯ ," IEEE Trans. ASSP, pp. 527-536, June 1985.

10. Paulraj, A., V.U. Reddy, T.J. Shan and T. Kailath, " Performance Analysis ..-," Proc. *of MILCOM*, pp. 41.5.1-41.5.5, 1986.
11. Reddy, V.U., A. Paulraj and T. Kailath, " Performance Analysis ···," *IEEE Trans.* on *ASSP*, pp. 927-936, July 1987.
12. Cornpton JR, R.T., " The Bandwidth ··· ," *IEEE Trans.* on *AP*, pp.5-14, January 1988.
13. Frost III, O.L.," An Algorithm ··· ," Proc. *IEEE*, pp. 926–935, August 1972.
14. Sam Shanmugarn, K., Digital and Analog Communication Systems, John Wiley & Sons, p. 513, 1979.

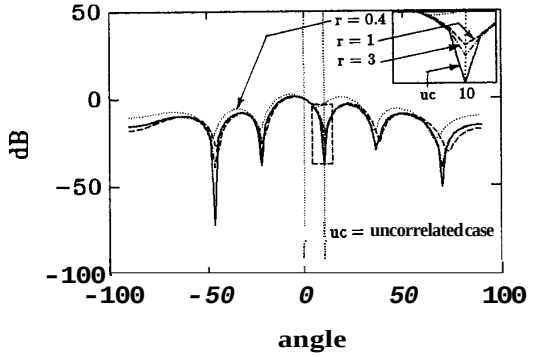

Fig. 2 Asymptotic beampatterns for different multipath delays ($M = 6$, $K = 4$, $B_d = 0.4$, $T_\alpha = 2\pi r/\Delta\omega$, SNR $= 10dB$, $\theta_d = 0^o$, $\theta_s = 10^o$)

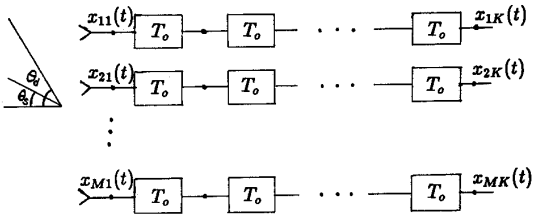

Fig. 1 A linear broadband array with M sensors and $(K-1)$ tap delays

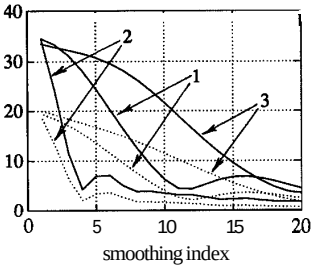

Fig. 3 Effect of progressive smoothing on the F-norm ($M = 6$, $K = 4$, $B_d = 0.4$, r = 0.4, $\sigma_d^2 = \sigma_s^2 = \sigma_v^2 = 1$)

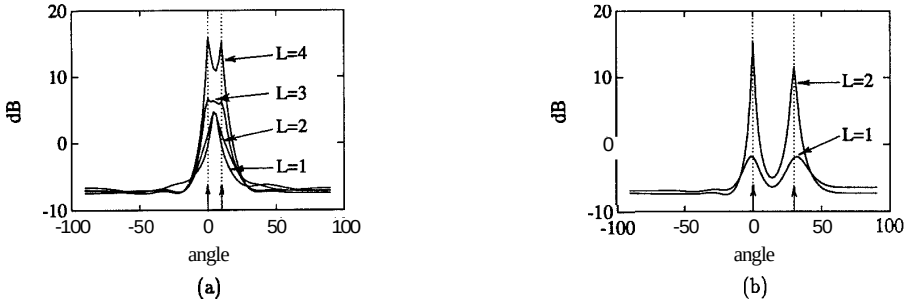

Fig. 4 Spatial spectra for different smoothing steps ($M = 6$, $K = 4$, $B_d = 0.4$, $r = 0.4$, no. of snapshots $= 200$)
(a) $\theta_d = 0^o$, $\theta_s = 10^o$ (b) $\theta_d = 0^o$, $\theta_s = 30^o$

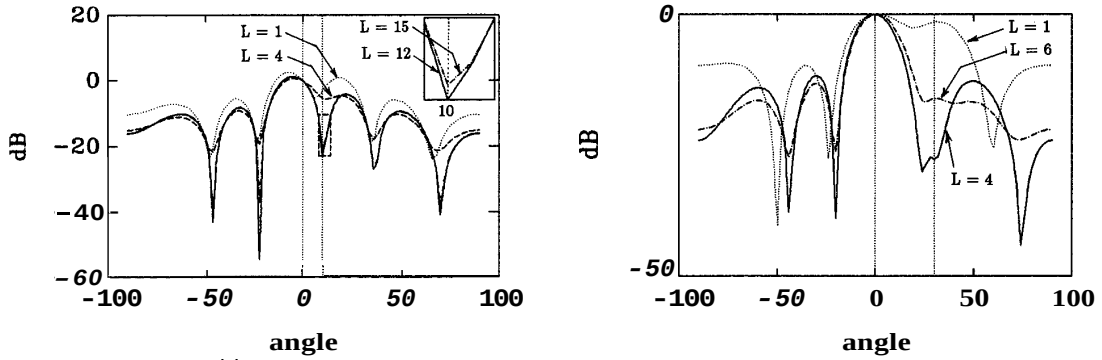

Fig. 5 Asymptotic beampatterns for different smoothing steps ($M = 6$, $K = 4$, $B_d = 0.4$, r = 0.4, $\sigma_d^2 = \sigma_s^2 = \sigma_v^2 = 10$)
(a) $\theta_d = 0^o$, $\theta_s = 10^o$ (b) $\theta_d = 0^o$, $\theta_s = 30^o$